

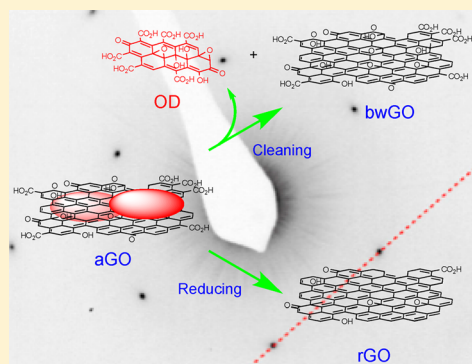
## Deoxygenation of Graphene Oxide: Reduction or Cleaning?

Helen R. Thomas,<sup>†</sup> Stephen P. Day,<sup>‡</sup> William E. Woodruff,<sup>‡</sup> Cristina Vallés,<sup>§</sup> Robert J. Young,<sup>§</sup> Ian A. Kinloch,<sup>§</sup> Gavin W. Morley,<sup>‡</sup> John V. Hanna,<sup>‡</sup> Neil R. Wilson,<sup>\*,‡</sup> and Jonathan P. Rourke<sup>\*,†</sup><sup>†</sup>Department of Chemistry, University of Warwick, Coventry, CV47AL, United Kingdom<sup>‡</sup>Department of Physics, University of Warwick, Coventry, CV47AL, United Kingdom<sup>§</sup>School of Materials, The University of Manchester, Oxford Road, Manchester, M13 9PL, United Kingdom

## Supporting Information

**ABSTRACT:** We show that the two-component model of graphene oxide (GO), that is, composed of highly oxidized carbonaceous debris complexed to oxygen functionalized graphene sheets, is a generic feature of the synthesis of GO, independent of oxidant or protocol used. The debris present, roughly one-third by mass, can be removed by a base wash. A number of techniques, including solid state NMR, demonstrate that the properties of the base-washed material are independent of the base used and that it contains similar functional groups to those present in the debris but at a lower concentration. Removal of the oxidation debris cleans the GO, revealing its true monolayer nature and in the process increases the C/O ratio (i.e., a deoxygenation). By contrast, treating GO with hydrazine both removes the debris and reduces (both deoxygenations) the graphene sheets.

**KEYWORDS:** graphene oxide, chemically modified graphene, oxidation debris, reduction, deoxygenation



## INTRODUCTION

Graphene has exceptional optoelectronic and physical properties, it is highly transparent, and it has supreme mechanical strength,<sup>1</sup> good thermal conductivity, and high charge mobility.<sup>2</sup> This makes it a desirable material in many different scientific fields and has prompted an unprecedented level of research and interest in recent years.<sup>3,4</sup> A diverse range of applications have been proposed for graphene, and each application utilizes and requires a different set of properties of graphene.<sup>5</sup> As a result, an equally diverse range of production techniques are required for graphene; progress in developing applications is reliant on progress in producing particular forms of graphene. Methods such as chemical vapor deposition (CVD) on comparatively cheap metal foils can produce high-quality graphene sheets suitable for (opto)-electronic applications,<sup>6</sup> but they are unsuitable for bulk manufacture of graphene for applications such as inks or as functional components in composites. Chemically modified graphene (CMG)<sup>7</sup> is an attractive alternative for such applications, as its production is readily scalable and the functional groups provide a convenient starting point for adding functionality through further reaction.

The most common production route for CMGs on a large scale is from graphene oxide (GO),<sup>8</sup> produced from the exfoliation of graphite oxide. The original report on graphite oxide came in 1859 from Brodie,<sup>9</sup> who used potassium chlorate in a sulfuric acid as the oxidant. Despite refinements from Staudenmaier,<sup>10</sup> chlorate based oxidations of graphite were prone to explosions, and it was the development of a permanganate based oxidation by Hummers<sup>11</sup> in 1958 that

reduced the hazards associated with synthesizing graphite oxide. The synthesis of graphene oxide starts with graphite powder, which, as it is cheap and available in large quantities, makes the oxidation method an ideal process for graphene applications where quantity is more important than absolute quality. However, despite more than a hundred years of research into graphite oxide and the intense recent research into GO, fundamental questions regarding the basic physical and chemical structure of GO still remain. These questions need to be addressed before applications of GO can be optimized.

Previously, we have shown that as-produced GO (aGO) made via a modified Hummers procedure actually comprises graphene-like sheets complexed with low molecular weight, highly oxidized, fragments.<sup>12</sup> As previously found for carbon nanotubes,<sup>13,14</sup> these organic fragments have been determined to be oxidation debris (OD). As also seen with the carbon nanotubes, it is possible to remove the OD by washing aGO with a basic solution, such as NaOH.<sup>15,16</sup> This leaves behind a black suspension of base washed GO (bwGO), which shows considerably reduced solubility in most common solvents. The effect of OD on the properties of GO can be quite dramatic as we,<sup>12,17</sup> and others,<sup>18–30</sup> have demonstrated.

In this paper, we look at using different synthetic protocols for aGO, bwGO, and OD in order to determine how the properties of these materials depend upon their synthesis. We

Received: February 26, 2013

Revised: July 24, 2013

Published: August 14, 2013

show that the two-component system of aGO is not specific to the Hummers method and that the properties of bwGO and OD are independent of the base used for the washing procedure. We find that hydrazine, a reagent commonly used for reducing GO, both removes the OD and reduces the graphene-like sheets.

## RESULTS AND DISCUSSION

**Comparing Oxidation Protocols.** Most researchers have found the Hummers<sup>11</sup> method (utilizing  $\text{KMnO}_4/\text{KNO}_3$  as the oxidant) to be the most convenient route to synthesizing GO. However, a substantial number of groups utilize the Brodie<sup>9</sup> route (with  $\text{KClO}_3$  as the oxidant) or its refinement by Staudenmaier,<sup>10</sup> and it is appropriate to investigate whether there are any substantive differences between the GO produced via the different routes. In particular, it is important to establish whether our observation of the presence of oxidation debris (OD) to the tune of approximately one-third by mass<sup>12</sup> is specific to the Hummers route.

Aqueous solutions of the GO formed via a chlorate oxidation and those from a permanganate oxidation look similar: both are golden brown. On evaporation, the materials are more easily distinguished: the chlorate material is noticeably lighter in color. Following a wash with aqueous  $\text{NaOH}$ , both materials darken substantially becoming dark brown/black, and it is possible to collect roughly one-third of the original mass as a very lightly colored OD from both. All characterization data collected indicated that the OD extracted from the as produced GOs (aGO) is independent of the method of synthesis.

Comparisons of the base-washed material (bwGO) produced in this manner also showed little difference in structure. Figure 1 shows a typical directly observed, magic angle spinning

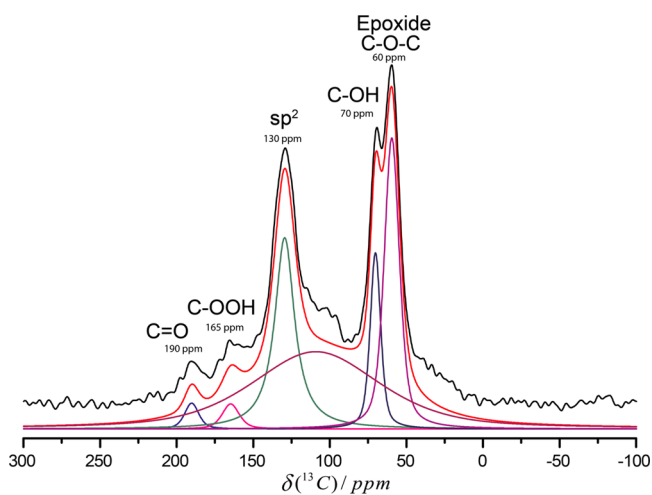


**Figure 1.**  $^{13}\text{C}$  solid state MAS NMR spectrum of GO as produced by the Hummers method acquired using single pulse (direct) observation of the  $^{13}\text{C}$  nucleus. The experimental spectrum (black line) has been deconvoluted into 6 components (5 individually labeled) with the red line representing the sum of those components.

(MAS), solid state  $^{13}\text{C}$  NMR (SSNMR) spectrum of Hummers aGO. The experimental spectrum has been fitted to the components assigned to the functional groups previously reported in GO,<sup>31,32</sup> and it is possible to clearly distinguish them all. An additional broad resonance centered at  $\delta \sim 110$  ppm is indicative of paramagnetically influenced  $\text{sp}^2$  carbon;<sup>33</sup>

EPR measurements (see SI) confirmed a strong paramagnetic response that could be correlated with this broad signal.

Figure 2 illustrates comparative solid state  $^{13}\text{C}$  NMR data associated with the Hummers and Brodie/Staudenmaier aGO

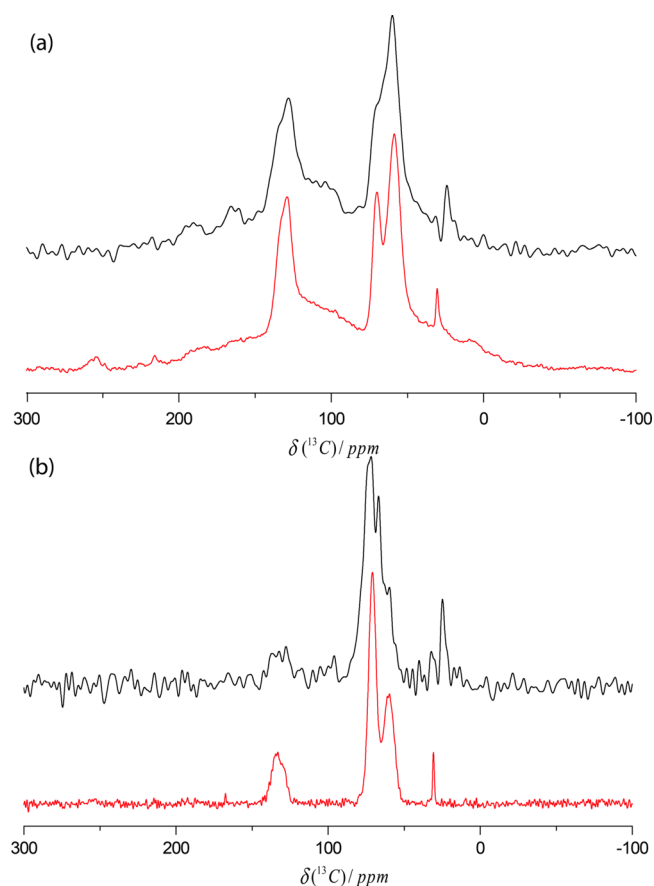


**Figure 2.**  $^{13}\text{C}$  solid state NMR data of aGO produced by the Hummers method (black spectra) and the Brodie/Staudenmaier method (red spectra). (a) Spectra acquired via direct single pulse  $^{13}\text{C}$  MAS observation. (b) Spectra acquired using a  $^1\text{H}$ - $^{13}\text{C}$  CPMAS experiment.

materials, with Figure 2(a) showing the directly observed  $^{13}\text{C}$  single pulse MAS spectra, while Figure 2(b) shows the corresponding  $^1\text{H}$ - $^{13}\text{C}$  cross-polarization (CPMAS) spectra. The solid state  $^{13}\text{C}$  NMR data for the two different samples are essentially the same (other than the signal-to-noise ratios). The  $^{13}\text{C}$  MAS and CPMAS data provide complementary structural information describing the GO surface and its functionalities; while the single pulse MAS experiment provides a semi-quantitative survey of all carbon species characterizing the system, the  $^1\text{H}$ - $^{13}\text{C}$  CPMAS experiment provides information on those carbon species in close proximity to attached protons.

If motional and exchange considerations can be neglected, the use of a  $^1\text{H}$ - $^{13}\text{C}$  Hartmann-Hahn (contact) period of  $\sim 1$ – $2$  ms should facilitate a maximum enhancement in  $^{13}\text{C}$  structural moieties situated 1–2 bond lengths away from  $^1\text{H}$  species, while more distant  $^{13}\text{C}$  species will experience much reduced enhancements.<sup>34</sup> As the dipolar interaction facilitating the  $^1\text{H}$ - $^{13}\text{C}$  cross-polarization process is a through-space phenomenon,  $^1\text{H}$ - $^{13}\text{C}$  contact can be established from intermolecular<sup>34</sup> and intramolecular<sup>35</sup> scenarios, thus implying that protonated molecules such as OD, which exhibit an interaction with the GO surface, can also contribute to the

CPMAS signal enhancement. It is expected that the predominant protonated species will be associated with hydroxyl groups directly bonded to the carbon network. If this is true then the signals of the carboxyl and deprotonated carboxylic acid functionalities, and the bulk of the  $sp^2$  network, are expected to diminish dramatically under  $^1\text{H}$ - $^{13}\text{C}$  cross-polarization conditions. A comparison of parts a and b of Figure 2 does indeed highlight these effects; in addition, a reduction in the intensity of the epoxide signal is also observed. Since this reduction in the epoxide signal intensity is of a similar order of magnitude to the reduction of the  $sp^2$  carbon species, this suggests that there is no linkage between the positions of the epoxide and hydroxyl groups on the GO surface.

Other spectroscopic techniques (e.g., FTIR, see SI) also show little difference between GO from the two different oxidants, and our observations are in keeping with a recent comparative study between GO formed by permanganate and chlorate oxidations, where the only observable differences were found to be a small increase in the carbonyl/carboxyl functionalities from the permanganate oxidations and a higher heterogeneous electron-transfer rate for chlorate produced GO.<sup>36</sup>

A recent refinement of the Hummers permanganate oxidation uses a reaction medium of 10% phosphoric acid/90% sulfuric acid (as opposed to 100% sulfuric for the “classic” Hummers) with no added  $\text{NaNO}_3$  and offers substantially reduced reaction times and increased yields as its principal benefits.<sup>37</sup> GO prepared via this route was also tested: washing with NaOH shows the presence of OD at 32% (see SI for spectra). Another more recent report identifies “pristine graphite oxide” (formed via a permanganate oxidation and an anhydrous workup) as a material that can be hydrolyzed to give conventional GO upon treatment with water.<sup>38</sup> Hydrolysis of samples of “pristine graphite oxide” initially collected via an ethyl acetate wash and work up gave a material that resembled conventional Hummers GO, and we found this material to be composed of 28% OD.

Thus, it appears that there are no significant differences in the GO formed from three different permanganate and the chlorate oxidation protocols. All key experiments reported in this paper were undertaken with both chlorate and permanganate GO, and as we observed no significant differences between them, we do not distinguish between them.

**Removing OD from GO.** In our earlier study, we had reported using sodium hydroxide at concentrations between 0.01 and 1 M to effect the base washing that removes the OD. From Figure 3, the difference between the directly detected (single pulse)  $^{13}\text{C}$  MAS NMR data of aGO and bwGO can be observed. The most obvious change is a large proportional increase of the  $sp^2$  network resonance ( $\delta \sim 130$  ppm) and the broader  $sp^2$  network resonance indicating interaction with delocalized electrons ( $\delta \sim 110$  ppm) relative to the resonances representing oxygen-related functionalities in the bwGO material. It is clear, therefore, that the base washing is highly effective at removing the OD material and that the bwGO still has the same oxygenated functionalities as aGO, but in much reduced concentrations.

A more subtle change is that the ratio of epoxides to hydroxides is lower in bwGO than in aGO. This could be the result of the OD containing a greater proportion of epoxides than are present on the graphene-like sheets of bwGO, or it might be that the base washing procedure itself is ring-opening epoxides to generate hydroxyls. We were unable to establish the

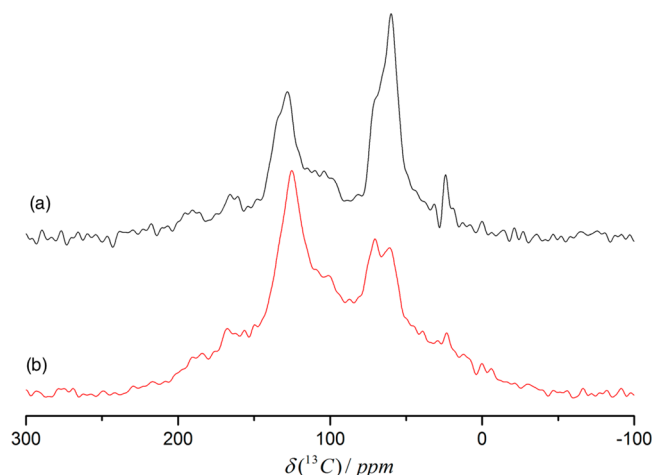


**Figure 3.** Comparison of directly detected  $^{13}\text{C}$  single pulse MAS NMR data from (a) aGO and (b) bwGO.

ratio of epoxide to hydroxide in OD (see both the solution and SSNMR spectra in SI), and thus, we are unable to distinguish between the two possibilities, but it is pertinent to note that the inherent instability of epoxides in GO has been observed spectroscopically and rationalized theoretically.<sup>20</sup>

Ammonia solutions (typically 0.45 molar) work equally well at removing the OD that is complexed to the GO sheets.<sup>39</sup> With equivalent preparation times (normally 30 min reflux), we could detect no differences between the bwGO sheets prepared this way, compared with those washed with NaOH—certainly, the FTIR (see SI), Raman (Figure 4), UV-vis, and  $^{13}\text{C}$

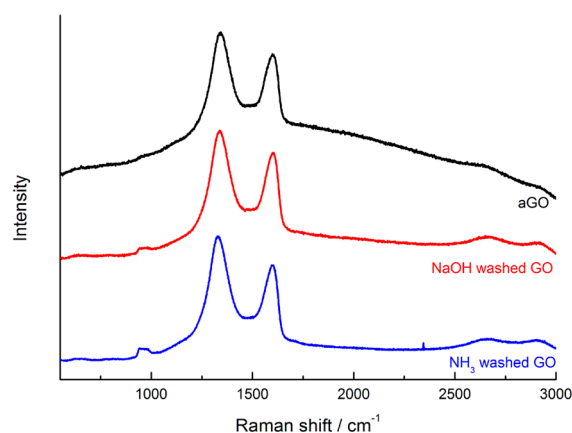


**Figure 4.** Raman spectra of aGO (top, black) and of bwGO, washed with NaOH (middle, red) or ammonia (bottom, blue), with an excitation wavelength of 633 nm. Fluorescence is seen for aGO (the broad, underlying, hump) but not for either form of bwGO.

SSNMR (see SI) were identical. The Raman spectra shown in Figure 4 highlight another feature of base washing that we have previously reported, the loss of fluorescence of GO that accompanies the removal of OD.<sup>17</sup>

The OD collected via an ammonia wash needs no subsequent neutralization because any excess ammonia is removed when the solvent is evaporated and dried under vacuum, though presumably, any carboxylic acids will now be present as the ammonium salt. By contrast, a significant quantity of NaOH (typically 90% of the sample by mass) remains when an NaOH wash is conducted. To simplify the

handling of these samples, we normally neutralize with aqueous HCl; consequently, samples collected via the NaOH washing contain significant quantities of NaCl (>95%). When a measured quantity of NaOH is used, it is possible to calculate the quantity of NaCl present in the final sample. The OD collected via an NaOH wash is normally slightly off white, while that from an ammonia wash is pale yellow.

The removal of the OD from the aGO results in a substantially reduced solubility of the bwGO in water and the other solvents typically used for processing GO (e.g., THF, ethanol), compared with the aGO.<sup>40</sup> We thus sought to find other solvents that might allow subsequent manipulation of the bwGO. A number of solvents have been tried and good solubility is exhibited in DMSO and DMF, but the most convenient we have found is an acetonitrile/water mix. Typically, stable dispersions of 0.3 mg/mL can be prepared by taking the still-wet freshly washed bwGO and dispersing into acetonitrile with gentle shaking. More concentrated solutions can then be obtained by evaporating solvent from these solutions. In terms of Hansen solubility parameters,<sup>41</sup> we generally find that acceptable solubility is found in solvents with a  $\delta_p$  of 13 or more (full results are given in the SI), compared with a  $\delta_p$  of 8 or more for aGO.<sup>42</sup>

Accurately assessing the C/O ratio in GO is difficult. X-ray photoelectron spectroscopy (XPS) is commonly used, but as a surface sensitive technique, it is prone to contamination through adsorbed adventitious carbon. Energy dispersive X-ray analysis (EDX) is less sensitive than XPS and due to the hygroscopic nature of GO is prone to contamination by adsorbed water (and so suggests more O than is actually present in the GO) but has a greater penetration depth and so is less sensitive to surface contamination and can be used in mapping mode to check for heterogeneities across samples. Here, we use EDX to track relative changes in composition: known reference samples were used for calibration. EDX analysis of the bwGO shows it to have a C/O ratio of (76:21) compared with (58:40) for the aGO, which is consistent with removal of highly oxygenated material.

**Structural Analysis of bwGO.** From a stable dispersion, bwGO can be controllably deposited on a range of substrates enabling further structural characterization. For TEM analysis, a drop of a solution of bwGO in acetonitrile/water was placed directly onto a lacy carbon support film. A representative TEM image and diffraction pattern are given in Figure 5. The bwGO sheets are almost electron transparent but can be discerned due to the occasional wrinkle or multiple overlapping sheets. The image shows that the structural integrity of the sheet is retained, with no evidence of damage (such as holes) or significant structural changes. The selected area electron diffraction (from the region indicated in Figure 5a) shows the presence of a single set of hexagonal diffraction spots as expected for a sheet with an ordered graphene-like structure. Analysis of the intensity of the diffraction spots shows that the inner  $hk = 10$  type spots are more intense than the outer  $hk = 11$  spots, proving that it is a single layer (i.e., graphene-like).<sup>43</sup> TEM of bwGO at this resolution is thus indistinguishable from TEM of aGO.<sup>44</sup>

bwGO sheets could be controllably and uniformly deposited on silicon oxide by spin coating from acetonitrile-bwGO dispersions. Figure 6 compares AFM analysis of aGO and bwGO, both deposited on silicon oxide. The images show sheets with a large range of lateral sheet sizes—the sheet size in aGO is dependent on the starting material and the way it is

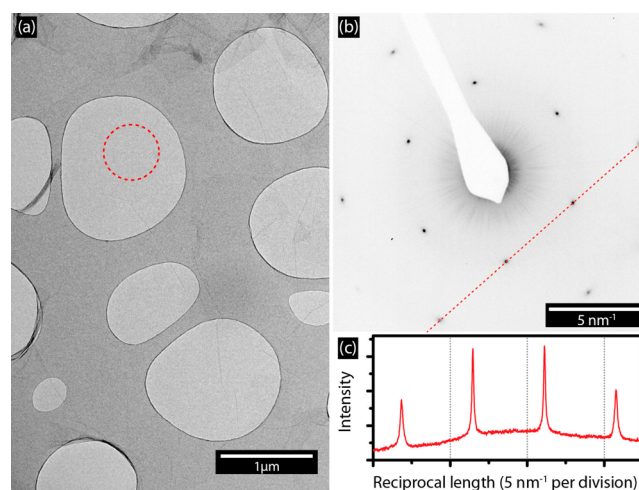


**Figure 5.** (a) Bright field TEM image of bwGO on a lacy carbon support. The dashed red circle in (a) indicates the area from which the electron diffraction pattern (b) was taken (note that the contrast has been inverted for clarity). (c) Intensity along the dashed red line in part b.

processed.<sup>45</sup> A comparison of parts a and b of Figure 6 shows that the additional processing required to obtain bwGO reduces the sheet size; this is to be expected, particularly due to the sonication used to redisperse the bwGO which is known to fragment the graphene oxide sheets,<sup>46</sup> and so, it does not suggest any significant chemical transformations in the graphene sheet. However, the typical sheet size for bwGO is still more than 1  $\mu\text{m}$  across. The AFM image of bwGO also demonstrates that it must form a stable dispersion in acetonitrile/water without coagulation as the sheets are flat on the silicon oxide surface with little aggregation.

Histograms of the height distributions of the images, Figure 6c and d, show distinct peaks due separately to the silicon oxide substrate, the first layer of aGO/bwGO, and multiple overlapping layers. From these histograms, the thicknesses of single sheets of aGO and bwGO on the substrate can be determined, as can their effective layer spacing. For aGO, we extract a first layer thickness of 1.2 nm, with a layer spacing of 1.0 nm. For bwGO, the first layer is 1.3 nm, with subsequent layers showing a spacing of 1.0 nm. The thickness of the aGO is consistent with previous reports for monolayers of aGO and is known to vary substantially depending, for example, on humidity.<sup>8</sup> AFM analysis thus shows that the aGO and bwGO are both fully exfoliated and consist of stable monolayer sheets in their dispersions.

Within the accuracy of these measurements, there is no evidence for a difference between the effective thickness of aGO/bwGO on silicon oxide, nor is there evidence for a difference between the layer spacing of aGO/bwGO. Note that previous reports have also observed an increased effective thickness of the first layer.<sup>47,48</sup> The increase in layer spacing relative to graphite cannot be explained merely by the length of the C–O bonds, and the similarity between the layer spacing of aGO and bwGO indicates that the OD does not increase the layer spacing. Instead, it is probable that the spacing between adjacent sheets is determined by the nanoscale distortions induced in the graphene-like backbone by the functional groups,<sup>49</sup> or as described by Mkhoyan et al.<sup>48</sup> ‘undulations arising from lattice distortions in the original atomic structure of the graphene sheets’. The large observed layer spacing can readily

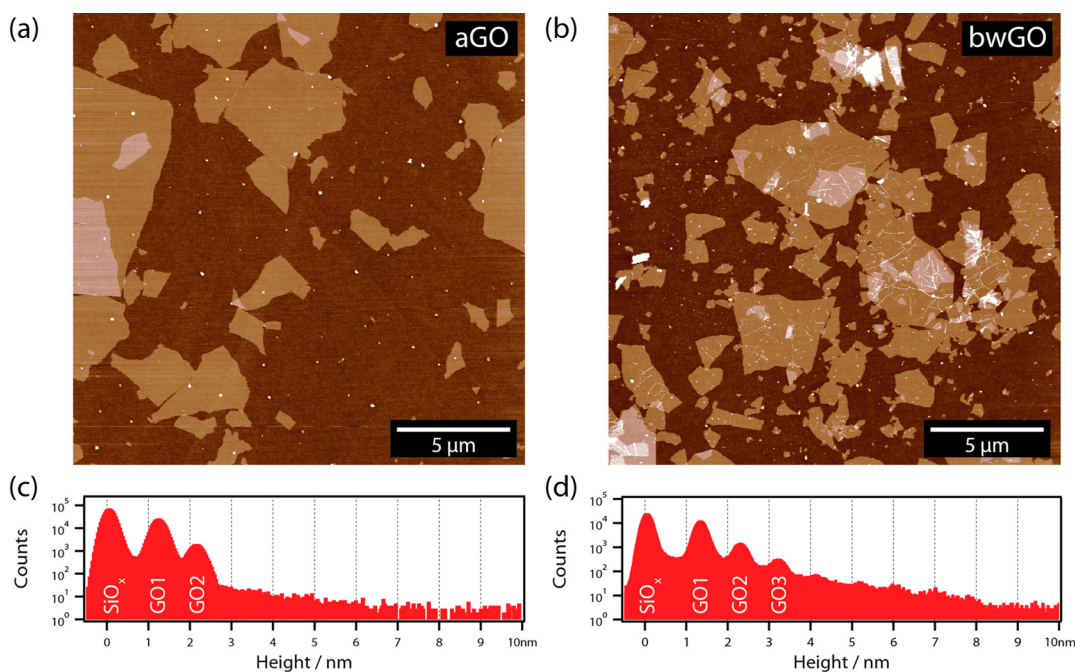


**Figure 6.** AFM topography images of (a) aGO and (b) bwGO, the full height scale in both images is 5 nm. (c, d) Histograms of the heights in parts a and b, respectively. The contributions of the silicon oxide substrate ( $\text{SiO}_x$ ), first layer of graphene oxide (GO1), second (GO2) and third layers (GO3) to the histogram are labeled.

accommodate OD between adjacent graphene-like sheets and so is consistent with the OD being complexed to the functionalized graphene in aGO. The similarity between measurements on aGO and bwGO indicates that the OD does not increase the layer spacing and is consistent with this picture that the layer spacing is dominated by the functionalization of the graphene-like sheets. The fact that there is no discernible change in layer spacing between the aGO and the bwGO suggests that the degree of functionalization of the graphene-like sheets does not change.

It is unsurprising that AFM does not resolve the presence or absence of OD on the graphene-like sheets. The expected lateral dimensions of the OD (likely to be  $<1$  nm) are small, and the coverage is high. From mass balance, about one-quarter of the surface has OD complexed to it, so the separation between OD fragments would be expected to be  $\sim 1$  nm, significantly less than the AFM tip diameter and hence lower than the lateral resolution of the AFM. At the same time, the expected thickness of the OD ( $\sim 0.5$  nm) is less than the roughness of the GO, again meaning that it is extremely unlikely to be resolved.

Both AFM and TEM show the graphene-like sheet to be continuous after base-washing, with the structural integrity intact. As a result, both AFM and TEM are consistent with the OD being initially complexed to the surface of the aGO and (considering the total mass of the OD) are not consistent with the OD being formed by excision of large regions from within the graphene sheet. Structural analysis by AFM and TEM thus shows that the graphene-like backbone of bwGO is similar to that previously discerned for aGO but does not yet resolve the OD.

**Chemical Characterization of OD.** As well as acting like a surfactant to solubilize GO, we have previously demonstrated that the OD is fluorescent, whereas the bwGO is not,<sup>17</sup> and similar results have been seen by other groups.<sup>19,50</sup> We have thus sought additional chemical characterization of this

material. The low molecular weight nature of OD has been established previously,<sup>12</sup> and repeated TEM and AFM investigations again confirmed this analysis: neither technique showed the presence of any sheet-like material in the OD.

Solution state NMR is an appropriate characterization technique for low molecular weight materials, but the OD is only appreciably soluble in water.  $^1\text{H}$  NMR spectra of OD in  $\text{D}_2\text{O}$  solvent reveal little: a broad resonance between 7.0 and 7.2 ppm is indicative of a large number of aromatic environments for the hydrogens. Carboxylic acid and alcohol protons would not be expected to show up in such a spectrum as these protons are readily exchanged for the NMR silent deuterium present in the solvent.  $^{13}\text{C}$  NMR spectra are more revealing: as well as sharp peaks at 162.8, 166.4, and 167.9, there is a broad peak at 170.3 ppm and a large underlying very broad peak between 180 and 160 ppm; a further very broad peak exists between 110 and 160 ppm (see SI). We can ascribe the broad peak between 160 and 180 ppm to be made up of multiple carboxyl carbon (esters, lactones and acids) resonances and can rule out the presence of ketones and aldehydes (expected chemical shift 190–210 ppm) in significant quantities. The broad peak between 110 and 160 ppm presumably arises from a large number of signals from aromatic type carbons (for instance, a simple benzene ring resonance is expected at 128 ppm, a benzene ring with a carboxyl group at 131 ppm, and one with an OH at 155 ppm). Thus, the solution NMR spectra are consistent with OD being a large number of different compounds with the same type of functional groups as aGO. The insolubility of the OD in solvents other than water is consistent with these observations: highly carboxylated materials would not be expected to be soluble in organic solvents. We also ran a solid state  $^{13}\text{C}$  NMR of the OD, and it was essentially no different from the solution spectrum (see SI).

While solution NMR will show the average composition, mass spectra will be dominated by compounds that readily

ionize and fly. Thus, a mass spectrum might show strong peaks that are actually only present in low proportions. With that caveat, we have recorded mass spectra using different ionization techniques, in particular, ESI and MALDI. Each technique gives a different result, but all techniques show ranges of signals between 200 and 900  $m/z$ , which can be assigned to a range of small, highly oxidized organic fragments; in some cases, accurate mass analysis allowed a formula to be assigned (see SI).

**Reducing GO.** One of the classic methods of reducing GO is with the use of hydrazine.<sup>51</sup> We have already noted that the use of NaOH can result in a deoxygenation,<sup>12</sup> and wondered if, as others have speculated,<sup>52</sup> one of the roles of the basic hydrazine is equivalent to the base-washing step.

Treatment of GO with hydrazine monohydrate solutions (0.5 molar) at room temperature for 3 h results in changed samples, with both aGO and bwGO producing very similar looking materials. The quantity of material produced is significantly different as ~150 mg of aGO produces ~100 mg of material, whereas only ~110 mg of bwGO is needed to produce ~100 mg of material; this is consistent with the hydrazine having a cleaning role and removing the OD. Spectroscopically, these new materials are very similar: there is a very substantial decrease in the intensity of the directly detected <sup>13</sup>C NMR signals of the epoxide, hydroxide, and carboxyl groups, relative to those of the sp<sup>2</sup> carbons, and this effect is apparent on samples of both aGO and bwGO, Figure 7a. The decrease in the intensity of these signals is considerably greater than that which arises from base washing (compare with Figure 3) and is mirrored by a change in the C/O ratio seen in the EDX (for the same sample treated sequentially, the ratios were 58:41 in aGO, 64:32 in bwGO and 70:30 in hydrazine reduced aGO). Thus, we can conclude that, in addition to removing OD, the hydrazine is genuinely reducing the GO.

More vigorous conditions (refluxing 1 h) is even more effective, and a 48 h reflux results in an almost complete removal of all oxygenated groups, Figure 7b, mirrored again by a further change in the C:O ratio to 77:23 for 1 h of reflux, 85:15 for 24 h reflux, and 91:8 for 48 h reflux. We should note, once again, the propensity of EDX to show O levels greater than expected, and if we consider the inaccuracies to be dominated by the hygroscopic nature of the material, we would expect the inaccuracies to become less significant as the reduction proceeds. Indeed, TGA analysis (SI) suggests the water content decreases by 25% upon base washing and 70% on reduction. Definitely though, nitrogen was not observed by EDX in any of the hydrazine treated samples, consistent with DFT studies of hydrazine de-epoxidation mechanisms that indicate that the only stable hydrazino alcohol intermediate are those that form from epoxide groups at the edges of the aromatic regions.<sup>53</sup> The mass loss on the essentially complete reduction of bwGO was around 20%, implying a C/O ratio of 4:1. TGA analysis (see SI) mirrors both the NMR and EDX findings, with decreasing quantities of material lost below 200 °C as the extent of reduction is increased; our most reduced material only shows mass loss above 600 °C.

## CONCLUSIONS

The presence of oxidation debris in as-produced graphene oxide is not a function of oxidation method: variants of both widely used oxidants give materials that contain roughly one-third highly oxidized low molecular weight material. The removal of this highly oxygenated OD from the aGO with base

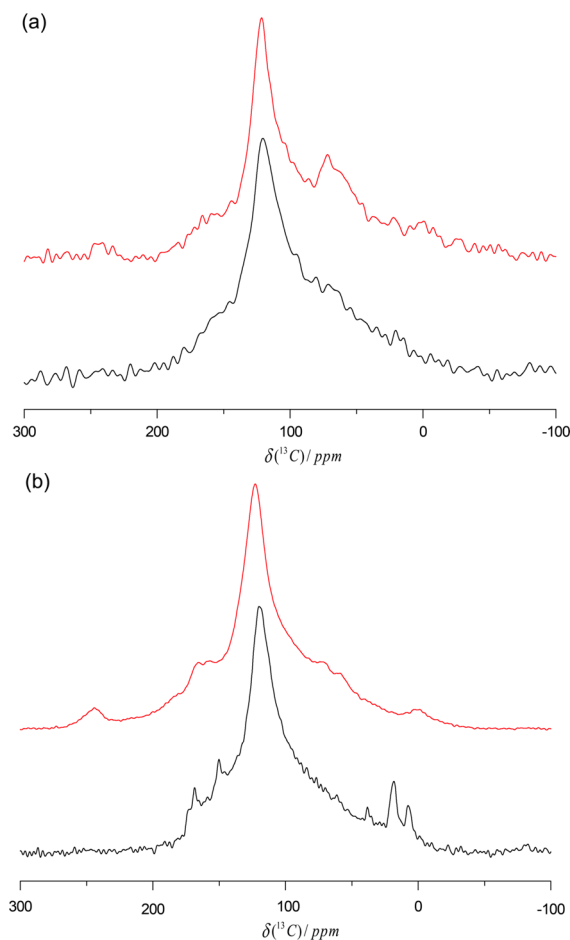
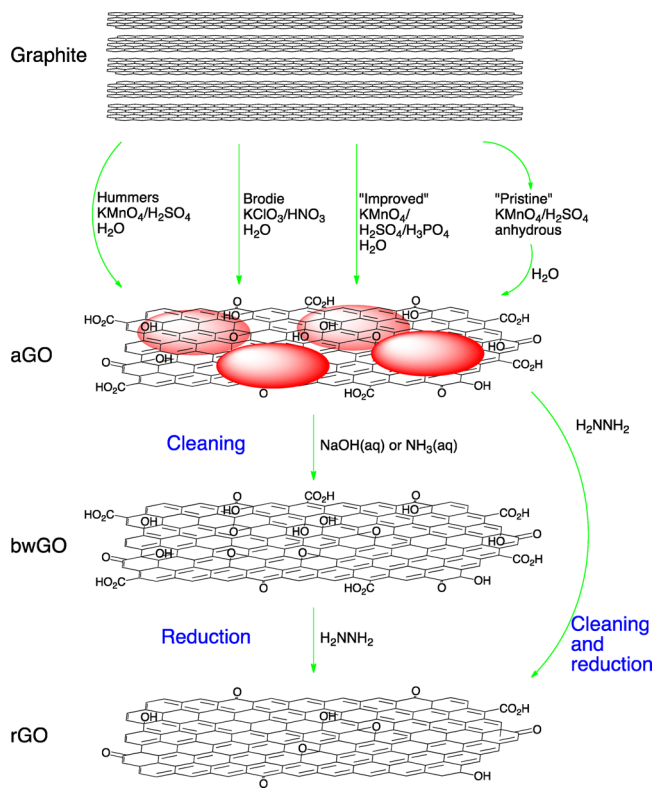


**Figure 7.** Directly detected <sup>13</sup>C single pulse MAS NMR spectra of hydrazine reduced GO. (a) Treatment of bwGO (top, red) and aGO (black, bottom) with hydrazine for 3 h at room temperature. (b) Treatment of bwGO with refluxing hydrazine for 1 h (top, red) and 48 h (black, bottom).

gives graphene-like sheets with a reduced oxygen content compared with the aGO. The cleaned version of GO so produced is shown by TEM to be a genuinely single sheet material, and AFM shows that it can be processed in much the same way as aGO, but without concerns about the presence of OD. If we revisit the literature, it becomes apparent that many researchers in the past have inadvertently removed the OD from their samples via washing or thermal treatments; indeed, one group postulated that it might simply be the basic nature of hydrazine that was responsible for its deoxygenating properties.<sup>54</sup> We have shown here that hydrazine both cleans the OD from the graphene-like sheets **and** reduces them, Scheme 1.

We can thus identify two important processes that can occur during treatment of graphene oxide: reduction and ‘cleaning’. The separation of highly oxidized material (the OD) from the bulk sample of aGO to give graphene-like sheets is ‘cleaning’; it reveals more of the true nature of graphene oxide. The graphene-like sheets are unchanged by this processing, but the resultant material, bwGO, has a lower level of oxygenation than aGO (an increase in the C/O ratio), and hence, deoxygenation has occurred. Since the graphene-like sheets are unaltered by the cleaning process, they have not themselves been reduced. True reduction of the GO requires reagents that add electrons to the graphene-like sheets, removing the directly bonded oxygen groups. A standard reducing reagent such as hydrazine

Scheme 1



cleans and reduces the graphene oxide, and this deoxygenation is thus the result of two separate processes, which, as we have demonstrated, can be performed sequentially. Correctly identifying and characterizing these deoxygenation processes will allow the improvement of functional properties in chemically modified graphenes, and those materials that are generated by the secondary oxidation of GO.<sup>55</sup>

## EXPERIMENTAL SECTION

**Instrumental Techniques.** Solid-state MAS NMR data were measured at an external field  $B_0$  of 9.4 T using a Bruker DSX-400 spectrometer operating at a <sup>13</sup>C Larmor frequency of 100.58 MHz. Both single pulse magic-angle-spinning (MAS) and cross-polarization, magic-angle-spinning (CPMAS) experiments were undertaken using a 4 mm Bruker double tuned probe in which MAS frequencies of 12 kHz were achieved. A sample of alanine was used to calibrate the <sup>13</sup>C MAS and <sup>1</sup>H–<sup>13</sup>C CPMAS experimental parameters; a Hartmann–Hahn contact period of 1 ms, an initial <sup>1</sup>H  $\pi/2$  pulse time of 4  $\mu$ s, a <sup>1</sup>H tppm decoupling strength during acquisition of ~100 kHz, and a recycle delay of 1 s were common to all CPMAS measurements. The single pulse experiments used a <sup>13</sup>C  $\pi/4$  pulse time of 2  $\mu$ s in conjunction with a recycle delay of 30 s. All <sup>13</sup>C chemical shifts are calibrated against a primary IUPAC reference TMS ( $\delta$  0 ppm) via a secondary alanine solid reference ( $\delta$ (CH<sub>3</sub>) 20.5 ppm,  $\delta$ (CH) 51.0 ppm,  $\delta$ (COOH) 177.8 ppm).

Raman spectra were recorded on a Renishaw 2000 spectrometer under 633 nm excitation.

EDX were recorded on a Zeiss SUPRA 55-VP FEGSEM with an EDAX Genesis analytical system, readings were taken in at least four random spots across a sample with the standard deviations in the mean values noted in parentheses. TEM measurements were recorded at 200 kV on a Jeol 2000FX with Gatan Orius camera. AFM measurements were recorded on an Asylum Research MFP3D-SA.

All samples were dried under on a Schlenk line (vacuum 0.1 Torr or better) at 60 °C until there was no further mass loss (typically 2 h).

**Synthesis. Hazard Warning.** Chlorate salts are known to be explosive and should be handled appropriately.

**Hummers Synthesis of GO.** Natural flake graphite (5.020 g) and KNO<sub>3</sub> (4.507 g) were suspended, with stirring, in concentrated sulphuric acid (169 mL). The mixture was cooled on ice, and KMnO<sub>4</sub> (22.443 g) was added over 70 min. The mixture was then allowed to warm to room temperature with constant stirring. After 24 h, the green solution had become too thick to stir. It was left for a further 4 days over which time there was a color change to purple. This mixture was slowly dispersed into 550 mL 5 wt % H<sub>2</sub>SO<sub>4</sub> in water over the course of 1 h and left to stir for a further 3 h. Hydrogen peroxide (45 mL, 30 vol, equivalent to 15g) was then added to the brown mixture over 5 min, with considerable effervescence, leaving a glittery gold suspension that was left stirring for 2 h. This suspension was then further diluted with 500 mL of 3 wt % H<sub>2</sub>SO<sub>4</sub>/0.5 wt % H<sub>2</sub>O<sub>2</sub> in H<sub>2</sub>O and left stirring for 12 h. The mixture was centrifuged (12500 rpm, 20 min), and the separated solid was collected, redispersed into 500 mL of 3 wt % H<sub>2</sub>SO<sub>4</sub>/0.5 wt % H<sub>2</sub>O<sub>2</sub> in H<sub>2</sub>O, and recentrifuged. In total, 6 such acidic washes were done, followed by 8 washes with pure water giving a neutral pH. After 3 washes, the glittery flakes had all disappeared leaving a much thicker, darker mixture. The resultant brown solution was dried under vacuum to give a brown film-like solid (5.0955 g).

EDX atomic % (standard deviation): C 58 (1); O 40 (2).

**Brodie Synthesis of GO.** Natural flake graphite (1.052 g) and potassium chlorate (8.523 g) were mixed together and cooled on dry ice to –20 °C. Fuming nitric acid (20 mL) was added slowly over 40 min with constant stirring. The mixture was then allowed to warm to room temperature and left stirring for 8 h. This green suspension was then heated to 60 °C and left stirring overnight, over which time there was a color change to blue. The suspension was centrifuged (12 500 rpm, 20 min), and the solid collected, washed with water, and recentrifuged. Drying under vacuum gave blue/silver flakes, which were mixed with potassium chlorate (8.517 g) and fuming nitric acid (20 mL) as before. After overnight stirring at 60 °C, the suspension was allowed to cool to room temperature, at which point it was left for a further 2 days under constant stirring. The mixture was then dispersed into water (100 mL) via sonication (20 min). A cloudy, brown solution was formed. A gold/brown flaky solid was extracted by centrifugation (12,500 rpm, 20 min), washed with water, and recentrifuged. The collected solid was dried under vacuum to give a gold-colored solid. Once again, this was mixed with potassium chlorate (8.523 g) and fuming nitric acid (60 mL). The mixture was stirred at room temperature for 12 h, then heated to 60 °C for 36 h, followed by a further 2 days at room temperature. The mixture was then dispersed into water (100 mL) via sonication (20 min) to form a creamy brown solution. A gold/brown flaky solid was collected by centrifugation (12,500 rpm, 20 min), washed with water, and recentrifuged. The solid was dried under vacuum to leave gold/brown flakes (1.043 g).

EDX atomic % (standard deviation): C 51 (2); O 45 (1); S 1.9 (1).

**"Improved" Synthesis of GO.**<sup>37</sup> Natural flake graphite (2.9860 g) and KMnO<sub>4</sub> (17.994 g) were dispersed into a 9:1 mixture of concentrated sulphuric acid (360 mL) and concentrated phosphoric acid (40 mL). The green suspension was heated to 50 °C and stirred for 15 h, by which point a thick purple mixture had formed. Once cool, the mixture was dispersed gradually into an ice cold solution of water (400 mL) and H<sub>2</sub>O<sub>2</sub> (3 mL, 30%). The mixture was centrifuged (12 500 rpm, 1 h), and the filtrate was washed successively with water (400 mL  $\times$  2), 30% HCl (400 mL, 11 M) and ethanol (400 mL  $\times$  6). After each washing, the supernatant was discarded and as much unreacted graphite was removed as possible. The resultant brown solution was dried under vacuum to give a brown film-like solid (1.7023 g).

EDX atomic % (standard deviation): C 58 (2); O 38 (1); S 2.8 (0.5).

**Synthesis of Hydrolyzed "Pristine" GO.**<sup>38</sup> Natural flake graphite (3.056 g) was suspended in concentrated H<sub>2</sub>SO<sub>4</sub> (400 mL). This was left stirring for 10 min before KMnO<sub>4</sub> (3.072 g) was added. The green, flaky mixture was left stirring at room temperature overnight, over which time there was a color change to purple.

More KMnO<sub>4</sub> (2.952 g) was added, turning the solution back to green within 5 min. After 6 h and a color change back to purple, more

KMnO<sub>4</sub> (3.048 g) was added. One last portion of KMnO<sub>4</sub> (3.048 g) was added after the mixture had been left stirring overnight. This was then left to stir over the weekend, resulting in a thick, purple mixture.

Ice cold water (90 mL) was added slowly followed by H<sub>2</sub>O<sub>2</sub> (0.5 mL). The pink mixture was centrifuged for 20 min, and the yellow supernatant was discarded. The pink solid was washed with ethyl acetate (400 mL), and the centrifuge cycle was repeated 6 times, by which point, the supernatant ethyl acetate was colorless. The extracted solid was dried under vacuum to give a pink solid. (16.434 g).

Some of this 'pristine' GO (0.2765 g) was dispersed in water (250 mL) via sonication. The resultant light brown solution was centrifuged (12 500 rpm, 15 min), and the collected brown solid was washed with water (400 mL × 2) and acetone (400 mL) before being dried under vacuum, leaving a dark brown solid (0.0436 g, 16%).

EDX atomic % (standard deviation): C 72 (1); O 27 (1).

**NaOH Wash of GO.** The same general method (as detailed below) was used for GO prepared via all routes:

**Hummers GO.** aGO (140 mg) was redispersed into H<sub>2</sub>O (250 mL) by mild sonication to form a stable light brown solution. NaOH was added (0.140 g), under constant stirring, to give a 0.014 M solution. There was immediate darkening on dissolution of the NaOH. The solution was then heated to 70 °C for 1 h. The resultant dark brown solution was centrifuged (12 500 rpm, 30 min) leaving a dark brown solid and colorless supernatant. This supernatant, and that of all subsequent centrifuge cycles, was collected. The dark brown solid was washed with water and re-centrifuged. The solid was reprotonated with dilute HCl (250 mL, 0.014 M) and stirred for 1 h at 70 °C. Once cool, the solid was collected as before and washed with water. The wet solid could then be dried under vacuum (0.1 Torr, 60 °C) to give a black solid (90.3 mg, 65%) or dispersed in a H<sub>2</sub>O/CH<sub>3</sub>CN mixture via sonication.

The collective supernatants were dried under vacuum to give an off-white powder (239.1 mg) of OD contaminated with NaCl (calculated to be 204.5 mg), that is, 34.6 mg (25%) of OD.

EDX atomic % (standard deviation): C 76 (1); O 21 (1); Na 1.9 (0.4); Cl 1.0 (0.1).

**Brodie GO.** 154.2 mg of GO gave 111.7 mg (72%) of a dark brown solid and OD as an off-white powder (258.0 mg) contaminated with NaCl (calculated to be 219.0 mg), that is, 39.0 mg (25%) of OD.

**"Improved" GO.** 196.2 mg of GO gave 120.6 mg (61%) of a dark brown solid and OD as an off-white powder (281.8 mg) contaminated with NaCl (calculated to be 219.0 mg), that is, 62.8 mg (32%) of OD.

EDX atomic % (standard deviation): C 76 (1); O 22 (1); Na 0.7 (0.3); Cl 0.4 (0.1).

**Hydrolyzed "Pristine" GO.** 107.2 mg GO gave 61.3 mg (57%) of a dark brown solid and OD as an off-white powder (234.6 mg) contaminated with NaCl (calculated to be 204.5 mg), that is, 30.1 mg (28%) of OD.

EDX atomic % (standard deviation): C 77 (2); O 18 (1); Na 1.1 (0.2); Cl 1.2 (0.4).

**Ammonia Solution Wash of GO.** The same general method (as detailed below) was used for GO prepared via both routes:

**Hummers GO.** 154 mg of aGO was redispersed in H<sub>2</sub>O (200 mL) to give a brown solution. The solution was stirred at room temperature, and excess ammonia (5 mL, 18.1 mol dm<sup>-3</sup>) was added. The mixture was then brought to reflux for 30 min. The mixture darkened appreciably but did not coagulate. Once cool, the mixture was centrifuged (12500 rpm, 3 h) to give separation into a black solid and pale yellow supernatant. The pale yellow supernatant was collected and re-centrifuged for 40 min. This left a small amount of brown residue and a colorless supernatant. The colorless liquid was dried under vacuum to give a pale yellow powder (34.3 mg, 23%). Meanwhile, the black solid was refluxed for 30 min with dilute HCl (0.01 M) and washed with water 3 times. The wet solid was collected and dried under vacuum (114 mg, 74%)

EDX atomic % (standard deviation): C 83 (0.1); O 17 (0.1).

**Brodie GO.** 100 mg gave 69 mg (69%) of black bwGO and 21 mg (21%) of OD as a pale yellow powder.

**Chemical Reduction of Hummers aGO.** Hummers aGO (148.0 mg) was redispersed in water (100 mL) and stirred at room

temperature. A solution of hydrazine monohydrate (5 mL, 12.8 mol dm<sup>-3</sup>) was added. The mixture was stirred at room temperature for 3 h, during which time it darkened appreciably. The mixture was centrifuged (12 500 rpm, 20 min) leaving a dark brown solid and colorless supernatant (which was discarded). The dark brown solid was collected, washed with water, and re-centrifuged (12 500 rpm, 30 min). It was then dried under vacuum to leave a black/silver flaky solid (102.1 mg).

EDX atomic % (standard deviation): C 70 (1); O 30 (1).

**Chemical Reduction of Brodie aGO.** Brodie aGO (101.0 mg) was redispersed in water (100 mL) and stirred at room temperature. A solution of hydrazine monohydrate (5 mL, 12.8 mol dm<sup>-3</sup>) was added. The mixture was heated at 70 °C for 1 h, during which time it darkened appreciably. The mixture was centrifuged (12 500 rpm, 30 min) leaving a dark brown solid and colorless supernatant (which was discarded). The dark brown solid was extracted, washed with water, and re-centrifuged (12 500 rpm, 30 min). It was then dried under vacuum (0.1 Torr, 60 °C) to leave a black/silver flaky solid (89.3 mg).

EDX atomic % (standard deviation): C 80 (1); O 18 (1).

**Chemical Reduction of Hummers bwGO.** A solution of hydrazine monohydrate (5 mL, 12.8 M) was added to a solution of Hummers bwGO in CH<sub>3</sub>CN (150 mL, 0.75 mg mL<sup>-1</sup>, 112 mg). The mixture was heated at 80 °C for 1 h. Once cool, the black mixture was centrifuged (12 500 rpm, 30 min) leaving a black solid and colorless supernatant (which was discarded). The black solid was collected, washed with water, and re-centrifuged (12 500 rpm, 30 min). It was then dried under vacuum to leave a flaky black solid (98.0 mg).

EDX atomic % (standard deviation): C 77 (1); O 23 (1).

Similarly, a sample was heated under reflux for 24 h.

EDX atomic %: C 85 (0.4); O 15 (0.4).

Similarly, a sample was heated under reflux for 48 h.

104 mg yield from 150 mg bwGO; EDX (atomic %): C 91 (2); O 8 (2).

## ■ ASSOCIATED CONTENT

### 📄 Supporting Information

Solution NMR spectra of OD, additional sets of solid state NMR (direct observe and CPMAS), FTIR spectra of all samples, TGA data, and mass spectra. This material is available free of charge via the Internet at <http://pubs.acs.org>.

## ■ AUTHOR INFORMATION

### Corresponding Authors

\*E-mail: [neil.wilson@warwick.ac.uk](mailto:neil.wilson@warwick.ac.uk).

\*E-mail: [j.rourke@warwick.ac.uk](mailto:j.rourke@warwick.ac.uk).

### Notes

The authors declare no competing financial interest.

## ■ ACKNOWLEDGMENTS

We thank EPSRC for a studentship award to H.R.T. and for support for C.V. and I.A.K. through the EPSRC Challenging Engineering grant "Delivering Graphene as an Engineering Material" EP/IO23879/1. We also thank EPSRC and the Integrated Magnetic Resonance CDT for a studentship and support for S.P.D. J.V.H. thanks EPSRC and the University of Warwick for partial funding of the solid state NMR infrastructure at Warwick and acknowledges additional support for this infrastructure obtained through Birmingham Science City: Innovative Uses for Advanced Materials in the Modern World (West Midlands Centre for Advanced Materials Project 2), with support from Advantage West Midlands (AWM) and partial funding by the European Regional Development Fund (ERDF). Mass spectrometry equipment used on this project was also funded with support from Advantage West Midlands (AWM) (part funded by the European Regional Development Fund). G.W.M. is supported by the Royal Society.



## ■ REFERENCES

- (1) Lee, C.; Wei, X. D.; Kysar, J. W.; Hone, J. *Science* **2008**, *321*, 385.
- (2) Huang, X.; Yin, Z.; Wu, S.; Qi, X.; He, Q.; Zhang, Q.; Yan, Q.; Boey, F.; Zhang, H. *Small* **2011**, *7*, 1876.
- (3) Novoselov, K. S. *Angew. Chem., Int. Ed.* **2011**, *50*, 6986.
- (4) Yao, J.; Sun, Y.; Yang, M.; Duan, Y. *J. Mater. Chem.* **2012**, *22*, 14313.
- (5) Novoselov, K. S.; Falko, V. I.; Colombo, L.; Gellert, P. R.; Schwab, M. G.; Kim, K. *Nature* **2012**, *490*, 192.
- (6) Li, X.; Cai, W.; An, J.; Kim, S.; Nah, J.; Yang, D.; Piner, R.; Velamakanni, A.; Jung, I.; Tutuc, E.; Banerjee, S. K.; Colombo, L.; Ruoff, R. S. *Science* **2009**, *324*, 1312.
- (7) Ruoff, R. S. *J. Mater. Chem.* **2011**, *21*, 3272.
- (8) Dreyer, D. R.; Park, S.; Bielawski, C. W.; Ruoff, R. S. *Chem. Soc. Rev.* **2010**, *39*, 228.
- (9) Brodie, B. C. *Philos. Trans. R. Soc. London* **1859**, *149*, 249.
- (10) Staudenmaier, L. *Ber. Dtsch. Chem. Ges.* **1898**, *31*, 1481.
- (11) Hummers, W. S.; Offeman, R. E. *J. Am. Chem. Soc.* **1958**, *80*, 1339.
- (12) Rourke, J. P.; Pandey, P. A.; Moore, J. J.; Bates, M.; Kinloch, I. A.; Young, R. J.; Wilson, N. R. *Angew. Chem., Int. Ed.* **2011**, *50*, 3173.
- (13) Salzmann, C. G.; Llewellyn, S. A.; Tobias, G.; Ward, M. A. H.; Huh, Y.; Green, M. L. H. *Adv. Mater.* **2007**, *19*, 883.
- (14) Wang, Z.; Shirley, M. D.; Meikle, S. T.; Whitby, R. L. D.; Mikhailovsky, S. V. *Carbon* **2009**, *47*, 73.
- (15) Verdejo, R.; Lamoriniere, S.; Cottam, B.; Bismarck, A.; Shaffer, M. *Chem. Commun.* **2007**, 513.
- (16) Fogden, S.; Verdejo, R.; Cottam, B.; Shaffer, M. *Chem. Phys. Lett.* **2008**, *460*, 162.
- (17) Thomas, H. R.; Vallés, C.; Young, R. J.; Kinloch, I. A.; Wilson, N. R.; Rourke, J. P. *J. Mater. Chem. C* **2013**, *1*, 338.
- (18) Faria, A. F.; Martinez, D. S. T.; Moraes, A. C. M.; Maia da Costa, M. E. H.; Barros, E. B.; Souza Filho, A. G.; Paula, A. J.; Alves, O. L. *Chem. Mater.* **2012**, *24*, 4080.
- (19) Hu, C.; Liu, Y.; Yang, Y.; Cui, J.; Huang, Z.; Wang, Y.; Yang, L.; Wang, H.; Xiao, Y.; Rong, J. *J. Mater. Chem. B* **2013**, *1*, 39.
- (20) Larciprete, R.; Fabris, S.; Sun, T.; Lacovig, P.; Baraldi, A.; Lizzit, S. *J. Am. Chem. Soc.* **2011**, *133*, 17315.
- (21) Ambrosi, A.; Chua, C. K.; Bonanni, A.; Pumera, M. *Chem. Mater.* **2012**, *24*, 2292.
- (22) Barkauskas, J.; Dakševič, J.; Juškėnas, R.; Mažeikienė, R.; Niaura, G.; Račiukaitis, G.; Selskis, A.; Stankevičienė, I.; Trusovas, R. *J. Mater. Sci.* **2012**, *47*, 5852.
- (23) Li, X.; Yang, X.; Jia, L.; Ma, X.; Zhu, L. *Electrochem. Commun.* **2012**, *23*, 94.
- (24) Swager, T. M. *ACS Macro Lett.* **2012**, *1*, 3.
- (25) Wajid, A. S.; Das, S.; Irin, F.; Ahmed, H. S. T.; Shelburne, J. L.; Parviz, D.; Fullerton, R. J.; Jankowski, A. F.; Hedden, R. C.; Green, M. *J. Carbon* **2012**, *50*, 526.
- (26) Young, R. J.; Kinloch, I. A.; Gong, L.; Novoselov, K. S. *Compos. Sci. Technol.* **2012**, *72*, 1459.
- (27) Giardi, R.; Porro, S.; Chiolerio, A.; Celasco, E.; Sangermano, M. *J. Mater. Sci.* **2013**, *48*, 1249.
- (28) Oh, J.-S.; Nguyen Dang, L.; Hwang, T.-S.; Hong, J.-P.; Lee, Y. K.; Nam, J.-D. *J. Mater. Sci.* **2013**, *48*, 1127.
- (29) Wang, J.; Jia, H.; Tang, Y.; Ji, D.; Sun, Y.; Gong, X.; Ding, L. *J. Mater. Sci.* **2013**, *48*, 1571.
- (30) Wang, Z.; Wang, W.; Wang, M.; Meng, X.; Li, J. *J. Mater. Sci.* **2013**, *48*, 2284.
- (31) Cai, W.; Piner, R. D.; Stadermann, F. J.; Park, S.; Shaibat, M. A.; Ishii, Y.; Yang, D.; Velamakanni, A.; An, S. J.; Stoller, M.; An, J.; Chen, D.; Ruoff, R. S. *Science* **2008**, *321*, 1815.
- (32) Gao, W.; Alemany, L. B.; Ci, L.; Ajayan, P. M. *Nat. Chem.* **2009**, *1*, 403.
- (33) Lukins, P. B.; McKenzie, D. R.; Vassallo, A. M.; Hanna, J. V. *Carbon* **1993**, *31*, 569.
- (34) Vassallo, A. M.; Hanna, J. V.; Wilson, M. A.; Lockhart, N. C. *Energy Fuels* **1991**, *5*, 643.
- (35) Hanna, J. V.; Wilson, M. A. *J. Phys. Chem.* **1992**, *96*, 6518.
- (36) Chua, C. K.; Sofer, Z.; Pumera, M. *Chem.—Eur. J.* **2012**, *18*, 13453.
- (37) Marcano, D. C.; Kosynkin, D. V.; Berlin, J. M.; Sinitskii, A.; Sun, Z.; Slesarev, A.; Alemany, L. B.; Lu, W.; Tour, J. M. *ACS Nano* **2010**, *4*, 4806.
- (38) Dimiev, A.; Kosynkin, D. V.; Alemany, L. B.; Chaguine, P.; Tour, J. M. *J. Am. Chem. Soc.* **2012**, *134*, 2815.
- (39) He, W.; Lu, L. *Adv. Funct. Mater.* **2012**, *22*, 2542.
- (40) Konkena, B.; Vasudevan, S. *J. Phys. Chem. Lett.* **2012**, *3*, 867.
- (41) Hansen, C. M. *Hansen Solubility Parameters: A User's Handbook*, 2nd ed.; CRC Press: Hoboken, 2007.
- (42) Park, S.; An, J.; Jung, I.; Piner, R. D.; An, S. J.; Li, X.; Velamakanni, A.; Ruoff, R. S. *Nano Lett.* **2009**, *9*, 1593.
- (43) Wilson, N. R.; Pandey, P. A.; Beanland, R.; Rourke, J. P.; Lupo, U.; Rowlands, G.; Römer, R. A. *New J. Phys.* **2010**, *12*, 125010.
- (44) Wilson, N. R.; Pandey, P. A.; Beanland, R.; Young, R. J.; Kinloch, I. A.; Gong, L.; Liu, Z.; Suenaga, K.; Rourke, J. P.; York, S. J.; Sloan, J. *ACS Nano* **2009**, *3*, 2547.
- (45) Zhang, L.; Liang, J.; Huang, Y.; Ma, Y.; Wang, Y.; Chen, Y. *Carbon* **2009**, *47*, 3365.
- (46) Pan, S.; Aksay, I. A. *ACS Nano* **2011**, *5*, 4073.
- (47) Jung, I.; Pelton, M.; Piner, R.; Dikin, D. A.; Stankovich, S.; Watcharotone, S.; Hausner, M.; Ruoff, R. S. *Nano Lett.* **2007**, *7*, 3569.
- (48) Mkhoyan, K. A.; Contryman, A. W.; Silcox, J.; Stewart, D. A.; Eda, G.; Mattevi, C.; Miller, S.; Chhowalla, M. *Nano Lett.* **2009**, *9*, 1058.
- (49) Wilson, N. R.; Pandey, P. A.; Beanland, R.; Rourke, J. P.; Lupo, U.; Rowlands, G.; Roemer, R. A. *New J. Phys.* **2010**, *12*, 125010.
- (50) Kozawa, D.; Miyauchi, Y.; Mouri, S.; Matsuda, K. *J. Phys. Chem. Lett.* **2013**, *4*, 2035.
- (51) Gao, X.; Jang, J.; Nagase, S. *J. Phys. Chem. C* **2009**, *114*, 832.
- (52) Fan, X.; Peng, W.; Li, Y.; Li, X.; Wang, S.; Zhang, G.; Zhang, F. *Adv. Mater.* **2008**, *20*, 4490.
- (53) Gao, X.; Jang, J.; Nagase, S. *J. Phys. Chem. C* **2009**, *114*, 832.
- (54) Fan, X. B.; Peng, W. C.; Li, Y.; Li, X. Y.; Wang, S. L.; Zhang, G. L.; Zhang, F. B. *Adv. Mater.* **2008**, *20*, 4490.
- (55) Radich, J. G.; Kamat, P. V. *ACS Nano* **2013**, *7*, 5546.